Two-Site Molecules as a Road for Engineering Complexity in Chemical Systems

L. Jullien,*,† A. Lemarchand,*,‡ S. Charier,† O. Ruel,† and J.-B. Baudin†

École Normale Supérieure, Département de Chimie, CNRS UMR 8640, 24 rue Lhomond, 75231 Paris Cedex 05, France, and Université Pierre et Marie Curie, Laboratoire de Physique Théorique des Liquides, CNRS UMR 7600, 4 place Jussieu, 75252 Paris Cedex 05, France

Received: March 17, 2003; In Final Form: June 9, 2003

Molecules that contain two coupled reactive sites are simple chemical systems that may nevertheless already exhibit some complex behaviors when they are subjected to suitable external constraints. This report first proposes a theoretical model and an experimental illustration to demonstrate that the introduction of an auxiliary reactive site on a substrate can lead to local and continuous tuning of the thermodynamic and kinetic properties of a reaction of interest. It is then shown that a similar kinetic scheme that is appropriate for describing the evolution of concentrations in a two-site catalysis exhibits diverse properties when maintaining the system far from equilibrium and varying the order of magnitude of the rate constants: tuning of chemical yield, autocatalysis, and kinetic proofreading are obtained.

1. Introduction

Beyond the extremely involved strategies that have been developed by living beings at the present step of evolution, this paper addresses the microscopic design of simple classes of molecular structures and external constraints that are engaged in minimal kinetic mechanisms such that the dynamical and asymptotic properties of the tailored system mimic at the macroscopic level the complex behaviors (such as reproduction, competition, or selection) that are encountered in biological organisms. Complexity is herein ultimately understood as the emergence of spatio-temporal organizations in open systems maintained out of equilibrium thanks to appropriate exchanges with the exterior.[1] From the latter point of view, different models that exhibit complex nonlinear behaviors have been already introduced.[1,2] Unfortunately, they do not necessarily allow the synthetic chemist to design minimal microscopic chemical structures. As an example related to molecular evolution, autocatalysis is often claimed to have had a major role in the emergence of self-organization of living beings whose metabolism relies on organic reactions.[1−3] However, simple autocatalytic reactions are essentially absent in organic chemistry, with the exception of a few isolated reactions, such as ester hydrolysis.[4] In fact, already-reported autocatalytic behaviors involve either collective phenomena such as phase transitions,[5,6] rather sophisticated structures that are inspired by the mechanism of DNA self-replication,[7−15] the formation of homomultimeric chelates,[16,17] or feedback mechanisms that are linked to physical properties.[18] Yet, the question of whether autocatalysis can emerge when simpler organic structures are involved still remains.

The existence and stability of an attractor, which is associated with a given asymptotic regime, are dependent on the parameter values of the dynamical system. In an open system, the parameters are of two different natures: the values of the first set are fixed by the exchanges with the exterior, whereas those of the second set characterize the properties of the system itself. In a living system, the parameters of the first set are imposed by the constraints that are exerted by the environment. In the case of an artificial chemical system, these parameters are, for example, the concentrations of the chemical species that often can be fixed by matter exchanges with ideal reservoirs. The parameters of the second type are the imposed rate constants of the different elementary steps of the chemical mechanism. To explore the diversity of possible behaviors of a given dynamical system, i.e., a given set of constraints and elementary reactions, we suggest the addition of new processes, which would involve new species of controlled nature and concentration, to play on the apparent value of the parameters that previously were fixed. The basic assumption on which our approach relies concerns the microscopic structure of the reactants considered. We propose that the structure, which consists of two different reactive sites on a same molecule, is one of the simplest molecular structures, already possessing enough potentialities to provide a rich collection of dynamical and asymptotic properties of a chemical system. Such an approach has some common features with the phenomenon of allostery, which is encountered in the living world[4] and was reproduced in artificial systems quite a long time ago.[19] Here, we deliberately introduce a second reactive site, coupled to the first one, to exert a certain amount of control on the reaction that involves the first site. The idea is to control the auxiliary reaction through exchanges with reservoirs to maintain constant concentrations of some of the species that are reacting on the second site. The intensity of the coupling between the two sites (i.e., the modification of the reactivity of a site, depending on the state of the other one) will determine the tuning range of the kinetic and thermodynamic properties of the reaction of interest.

The paper is organized as follows. In section 2, the macroscopic behaviors of reactant molecules that contain either one or two coupled reactive sites are compared. The two-site strategy is used to tune the thermodynamic and kinetic features of the first reaction, with respect to the case of a unique reactive site,

* Authors to whom correspondence should be addressed. E-mail: Ludovic.Jullien@ens.fr (for L.J.), anle@lptl.jussieu.fr (for A.L.).

† École Normale Supérieure, Département de Chimie, CNRS UMR 8640.

‡ Université Pierre et Marie Curie, Laboratoire de Physique Théorique des Liquides, CNRS UMR 7600.

10.1021/jp030335d CCC: $25.00
Published on Web 08/14/2003

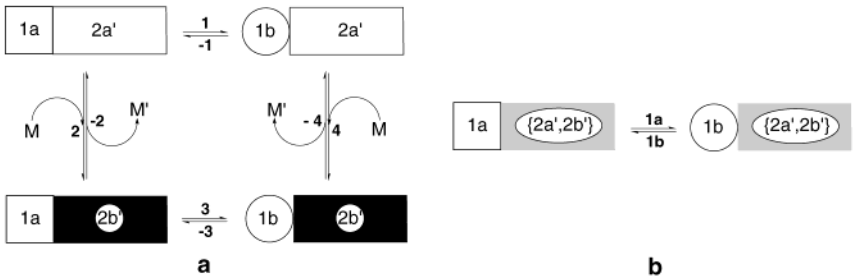

Figure 1. Scheme depicting the exchange processes involved in tuning kinetic and thermodynamic properties of reactions using two-site reactants. The scheme implies that two coupled sites (1 and 2) respectively exist under two states (a and b, and a' and b') (a) in its general form and (b) in its reduced form for {R, R′} and {P, P′} in a regime of fast exchange. In relation to the present model: $1a2a' = R$, $1b2a' = P$, $1a2b' = R'$, and $1b2b' = P'$.

but within the limits prescribed by equilibrium thermodynamics; in fact, the number of constraints imposed on the system does not prevent it from relaxing toward an equilibrium state, even when autocatalysis is transiently observed. Some theoretical predictions are illustrated by an experiment that involves the photoisomerization of 2,2′-azopyridine. It is shown, in particular, that protonation occurring at one pyridine can be used to tune the amount of cis versus trans isomers, under the given conditions of illumination. Considering still molecules with two reactive sites and reservoirs of species engaged in a reaction at the second site, section 3 illustrates the new kinetic and thermodynamic features of the reaction of interest that manifest when the system is maintained far from equilibrium. By analogy with allosteric enzymes[3] that are known to have a major role in the metabolism of living beings, we now assign to the two-site molecule the role of a catalyst and build a minimal kinetic model that involves a two-site catalysis. Keeping the same simple kinetic mechanism and changing only the parameter values (i.e., the concentrations that are fixed by the reservoirs and the rate constants), diverse properties that are presented by the system have been explored, including some sophisticated strategies that are observed in biology. Section 4 is devoted to the discussion of coupling that could be typically observed for small molecules. The conclusion is given in section 5.

2. Tuning the Kinetic and Thermodynamic Properties of Reactions Using Two-Site Reactants

Chemical species are often depicted as microscopic entities, in reference to bonds between atoms. In fact, any such considered "pure" species is a mixture that must be envisaged as an average, for instance, over an ensemble of conformations that individually exhibit specific reactivities.[20] More generally, a chemical species is better modeled as an average over a set of states $\{s_i\}$ that are interconverting rapidly along a collection of processes $s_i \rightleftharpoons s_j$.[2,21−23] Under these conditions, the kinetic mechanism and the rate-constant values characterize the species. In the present context, the basic idea to tune the parameters that characterize a reaction is to introduce a second site on the reactant and product that will be engaged in another reaction. Tunability will be exerted because of the species that are reacting with the second site.

2.1. The Model. A two-site reactant is considered:

$$1a \underset{k_{1b}}{\overset{k_{1a}}{\rightleftharpoons}} 1b \tag{1}$$

where $1a$ and $1b$ define the state of the site of interest, regardless of the state of the second site. Ignoring the state of site 1, the pilot reaction that affects site 2 is written as

$$2a' + M \rightleftharpoons 2b' + M' \tag{2}$$

Considering the different combinations that result from exchanges between the states a and b at site 1, and between the states a' and b' at site 2, the general form of the actual mechanism is given as

$$R \underset{k_{-1}}{\overset{k_1}{\rightleftharpoons}} P \tag{3}$$

$$R + M \underset{k_{-2}}{\overset{k_2}{\rightleftharpoons}} R' + M' \tag{4}$$

$$R' \underset{k_{-3}}{\overset{k_3}{\rightleftharpoons}} P' \tag{5}$$

$$P' + M' \underset{k_{-4}}{\overset{k_4}{\rightleftharpoons}} P + M \tag{6}$$

where $R = 1a2a'$, $P = 1b2a'$, $R' = 1a2b'$, and $P' = 1b2b'$. The simultaneous change of state for two sites, which is considered to be highly improbable, has been ignored. The kinetic mechanism is depicted in Figure 1a.

Coupling between sites 1 and 2 implies that the reactivity of site 1 is dependent on the state of site 2. Consequently, the values of the rate constants k_1 and k_3 are different in general. In particular, they differ a priori from the rate constant k_a of the reference reaction 7 that is exhibited by the corresponding one-site molecules:

$$a \underset{k_b}{\overset{k_a}{\rightleftharpoons}} b \tag{7}$$

Similarly, k_{-1} may be different from k_{-3} and k_b. For the sake of simplicity, we have chosen the following: $k_1 < k_3$ and $k_{-1} = k_{-3}$. In section 4, we return to discussion of the different couplings that can be implemented in the standard organic synthesis of two-site molecules. Typically, up to 3 orders of magnitude between k_1 and k_3 may be easily obtained.

In the special case of appropriate reactions 1 and 2, the state $1b$ (or, correspondingly, $1a$) from reaction 1, which originates from a modification of a given reactive group, may participate as a reactant (or, correspondingly, as a product) in reaction 2, involving the other reactive group. The following cross behavior is then observed:

$$2a' + 1b \rightleftharpoons 1a + 2b' \tag{8}$$

Considering the location of the reactive groups and considering all the processes that are acting on a given site, regardless of the state of the second site, now leads to the following relationships:

$$R \underset{k_{-1}}{\overset{k_1}{\rightleftharpoons}} P \tag{9}$$

$$R + P \underset{k_{-2P}}{\overset{k_{2P}}{\rightleftharpoons}} R' + R \tag{10}$$

$$R + P' \underset{k_{-2P'}}{\overset{k_{2P'}}{\rightleftharpoons}} R' + R' \tag{11}$$

$$R' \underset{k_{-3}}{\overset{k_3}{\rightleftharpoons}} P' \tag{12}$$

$$P' + R \underset{k_{-4R}}{\overset{k_{4R}}{\rightleftharpoons}} P + P \tag{13}$$

$$P' + R' \underset{k_{-4R'}}{\overset{k_{4R'}}{\rightleftharpoons}} P + P' \tag{14}$$

where the couples (P, P′) and (R, R′) respectively play the role that was assigned to M and M′ in reactions 3−6.

It is now possible to make the goals of the present section precise. First, we want to determine a domain in the control parameter space, {M, M′}, where the reactants R and R′ (or, correspondingly, the products P and P′) are exchanged in a sufficiently rapid manner to be considered as a single chemical species. The relevant concentration variables can be then defined:

$$1a(t) = R(t) + R'(t)$$
$$1b(t) = P(t) + P'(t) \tag{15}$$

whose dynamical evolution is given by the reduced mechanism of reaction 1. Whereas the rates k_a and k_b of the reaction of reference given in reaction 7 are imposed, it will be shown that the two control parameters M and M′ can be used to tune (i) the equilibrium value of the apparent yield $1b(\infty)/1a(\infty)$ and (ii) the value of the apparent rates k_{1a} and k_{1b}. Second, it will be illustrated that the model of two-site reactants can also result in autocatalysis when reactions 1 and 2 are involved in a cross behavior.

2.2. Theoretical Predictions. In the following two subsections, the concentrations of species M and M′ (denoted M and M′), are supposed to be constant and are imposed at will by appropriate reservoirs. This constraint does not exist anymore in the third subsection.

2.2.1. Thermodynamic Analysis. We are more specifically interested in tuning the value of the apparent yield of the reaction involving site 1 that can be evaluated by the ratio $(P(\infty) + P'(\infty))/(R(\infty) + R'(\infty))$. Indeed, this criterion measures the amount of state 1*b* versus state 1*a*, regardless of the state of site 2. The steady state that is attained by the open system in the large time limit obeys a detailed balance: the exchanges with the reservoirs stop by themselves and each reaction given in reactions 3−6 reaches thermodynamic equilibrium (see Supporting Information). This property significantly simplifies the analytical expression of the stationary state reached by the system. One finds

$$\frac{P(\infty) + P'(\infty)}{R(\infty)+R'(\infty)} = \frac{K_1}{K_4}\left(\frac{M + K_4 M'}{K_2 M + M'}\right) \tag{16}$$

where the K_i designate the thermodynamic constants ($K_i = k_i/k_{-i}$). Note that (i) the relevance of the notion of species for the two sets of compounds {R, R′} and {P, P′}, and (ii) the interpretation of the ratio $(P(\infty) + P'(\infty))/(R(\infty) + R'(\infty))$ as the apparent yield of the reaction require conditions on the kinetics of exchange between the compounds of each set that are addressed in the next subsection. The ratio $(P(\infty) + P'(\infty))/(R(\infty) + R'(\infty))$, plotted as a function of M and M′, is given in Figure 2a. It reaches limit values that are respectively equal to the equilibrium constants associated with reactions 3 and 5: the ratio tends to K_3 at high M and low M′, whereas it tends to K_1 at low M and high M′. The transition between both extreme regimes is induced by a variation of the concentrations M and/or M′ over ∼2 orders of magnitude. The locus of inflection points is located on the straight line of equation $M'/M = K_2$ that defines a threshold. In fact, two different situations occur, depending on the rates of the reactions that determine the weights of the reactions 3 and 5 to form 1*b* from 1*a* in the

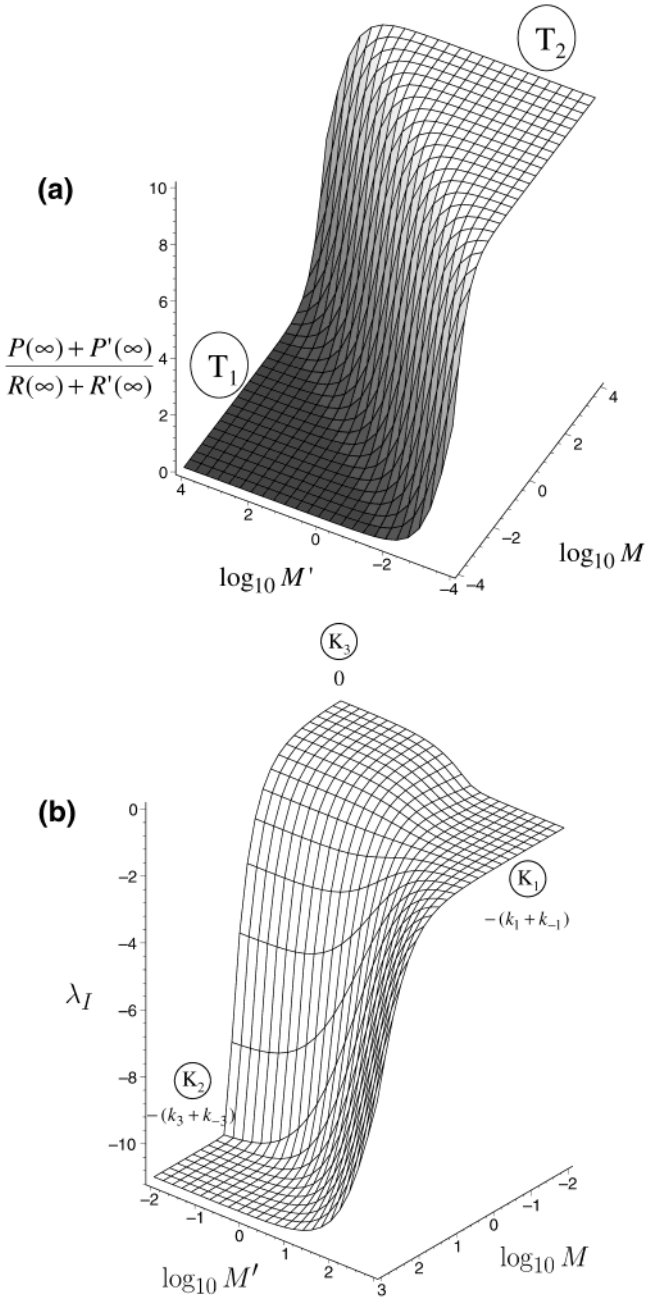

Figure 2. Three-dimensional plots: (a) the tuning reaction yield, plotted in the form of the ratio $(P(\infty) + P'(\infty))/(R(\infty) + R'(\infty))$ as a function of log M and log M′ for typical rate-constant values $k_1 = 0.1$, $k_{-1} = 1$, $k_2 = 1$, $k_{-2} = 1$, $k_3 = 10$, $k_{-3} = 1$, $k_4 = 0.1$, $k_{-4} = 10$; and (b) the tuning kinetic properties, plotted in the form of λ_I as a function of log M and log M′ for the same rate constants as those in panel a. In both situations, the concentrations of M and M′ are varied independently. (See Text and Supporting Information.)

steady state. In the domain T1, where $M'/M \gg K_2$, $(P(\infty) + P'(\infty))/(R(\infty) + R'(\infty))$ is controlled by reaction 3 and is equal to K_1. In contrast, in the domain T2, where $M'/M \ll K_2$, reaction 5 determines the asymptotic behavior and $(P(\infty) + P'(\infty))/(R(\infty) + R'(\infty)) = K_3$.

Thus, the deliberate introduction of an auxiliary reactive site coupled to the site of interest brings a significant advantage, in regard to the thermodynamical properties. Instead of being fixed at $b(\infty)/a(\infty) = k_a/k_b$, as for the reference system submitted for reaction 7, the yield $1b(\infty)/1a(\infty)$ can be continuously tuned between K_1 and K_3, according to the external constraints (here, the concentrations M and M′).

2.2.2. Kinetic Analysis. We now examine the control over the kinetic features of the present linear system that are discussed in relation to its eigenvalues λ and its eigenvectors (which define the characteristic relaxation times $1/|\lambda|$ and the corresponding eigenconcentrations). The results are more easily analyzed, in relation to the four eigenvalues $\lambda_i = -(\kappa_i + \kappa_{-i})$ $(i = 1-4)$ that originate from every process (reactions 3−6), considered individually (for $i = 1$ and 3, $\kappa_i = k_i$ and $\kappa_{-i} = k_{-i}$, whereas for $i = 2$ and -4, $\kappa_i = k_i M$ and $\kappa_{-i} = k_{-i} M'$). (See Supporting Information.)

As M and M′ vary, one expects two different types of kinetic regimes, depending on whether a partial equilibrium is first reached by reactions 3 and 5 (i.e., between R and P, and R′ and P′) or by reactions 4 and 6 (i.e., between R and R′, and P and P′). In the first case, the largest eigenvalue associated with the eigenconcentration $C_I = R(t) + P(t)$ obeys the relation $\lambda_I = -(k_{\{R,P\}} + k_{\{R',P'\}})$ with $k_{\{R,P\}} = [(k_{-1}k_2 + k_1k_{-4})/(k_1 + k_{-1})]M$ and $k_{\{R',P'\}} = [(k_{-2}k_{-3} + k_3k_4)/(k_3 + k_{-3})]M'$ (see Supporting Information). λ_I vanishes as M and M′ both approach zero. The two other nontrivial eigenvalues control the kinetics of the fast reactions 3 and 5 and are given by $\lambda_{II} = \max(\lambda_1, \lambda_3)$ and $\lambda_{III} = \min(\lambda_1, \lambda_3)$. The corresponding control parameter domain in the {M, M′} space, denoted as K3, is defined by the condition $\lambda_{II} \ll \lambda_I$, which selects sufficiently small values of M and M′. In domain K3 of Figure 2b, both R and R′, and P and P′ are in a regime of slow exchange and the experimentalist only controls the relative proportions in R and R′, and in P and P′. In the second case, observed as soon as either M or M′ is not too small, the exchange between R and R′, and between P and P′ can be considered fast, so as to envisage {R, R′} and {P, P′} (or similarly $1a$ and $1b$ in reference to reaction 1) as meaningful chemical species. The corresponding reduced mechanism is displayed in Figure 1b. The largest eigenvalue, which is associated with the eigenconcentration $C_I = 1a(t)$, is given by $\lambda_I = -(k_{1a} + k_{1b})$, where

$$k_{1a} = \frac{k_2k_3M + k_1k_{-2}M'}{k_2M + k_{-2}M'}$$

$$k_{1b} = \frac{k_{-3}k_{-4}M + k_{-1}k_4M'}{k_{-4}M + k_4M'} \qquad (17)$$

The two other eigenvalues control the kinetics of the fast reactions 4 and 6 and are given by $\lambda_{II} = \max(\lambda_2, \lambda_4)$ and $\lambda_{III} = \min(\lambda_2, \lambda_4)$ (see Supporting Information). The slowest relaxation time, characterized by $-1/\lambda_I$, is now determined by the processes of interest, i.e., reactions 3 and 5. As shown in Figure 2b, the domain of control parameter space {M, M′} where reactions 4 and 6 are fast may be split into two parts, denoted as K1 and K2. At sufficiently low M and large M′ (domain K1), the largest eigenvalue λ_I approaches λ_1: the slow relaxation mode is imposed by reaction 3. In contrast, λ_I approaches λ_3 for low M′ and sufficiently large M (domain K2): there, reaction 5 determines the slow regime. As also observed during the analysis of the thermodynamic features, the transition between domains K1 and K2 occurs over a change of the concentrations of M and M′ by <2 orders of magnitude.

We are now able to complete the conclusions drawn after the thermodynamic analysis. If the concentrations M and M′ are both small, i.e., in domain K3 of Figure 2b, one only controls the relative proportions in R and R′ (or, correspondingly, P and P′). In the remaining portion of parameter space {M, M′}, R and R′ (P and P′, correspondingly) are in a regime of fast exchange, with respect to the rate of reaction 3 or 5. The large domain of {M, M′} where {R, R′} and {P, P′} behave as individual chemical species covers the two domains T1 and T2, which are associated with the two extreme thermodynamical behaviors. By adjusting the values M and M′, we can continuously tune (i) the yield of the reaction of interest, according to eq 16 and (ii) its rate constants, as shown in eq 17. Going from domain K1 to domain K2 of Figure 2b, the largest relaxation time, $\tau_I = -1/\lambda_I$, can be tuned between $(k_1 + k_{-1})^{-1}$ and $(k_3 + k_{-3})^{-1}$, instead of being fixed at $(k_a + k_b)^{-1}$ in the reference system. Similarly, the rate constants to convert the *a* state to the *b* state (or the *b* state into the *a* state) can be changed from k_1 to k_3 (or from k_{-1} to k_{-3}) instead of being fixed at k_a (or k_b).

Such an approach may be useful to generate chemical species that exhibit rate constants that lie in precise ranges of values. From the latter point of view, a random search would be rather prohibitive if the corresponding ranges are narrow;[24] too many compounds would have to be synthesized. In contrast, the use of an auxiliary site grafted on the reactant of interest is an efficient way to tune the apparent values of the rate constants of a chemical reaction. Indeed, the use of auxiliary elements such as the present second reactive site is already not uncommon to the preparative chemists; covalently bound chiral auxiliaries are, for instance, used for chiral induction.[25]

2.2.3. Autocatalysis. Reactions 9−14 can be used to demonstrate that the present model also contains autocatalysis when the cross behavior (reaction 8) is observed. Starting from pure R, two pathways may be used to form P or P′, either (i) directly from reaction 9 or (ii) via an alternate pathway that involves an intermediate species such as R′ from reaction 10, which manifests itself when the concentration of P is sufficient. Autocatalysis can be revealed by noting that R and R′ share the same status as *a*, with respect to site 1, and can be considered as a single species that is denoted by $1a$ in a regime of fast exchange. Under analogous conditions on kinetics, P and P′ can be both denoted by $1b$. With these notations, reactions 10 and 11 and reactions 13 and 14 express the autocatalytic role of species $1a$ and $1b$. For the chosen set of rate constants, Figure 3 displays the typical sigmoidal, explosive kinetics, starting from pure R. The induction period, which is associated with relaxation according to reaction 9, is characterized by a slow dynamics. When the concentration of P reaches a threshold, the latter regime is followed by a rapid evolution toward the final state, using the alternate fast reactive channels that involve R′.

As a partial conclusion of the present section, a possible answer about the microscopic structure of elementary molecules that exhibit suitable features to favor both an increase of molecular diversity and the emergence of autocatalytic behaviors is, thus, the existence of two coupled sites that carry reactive groups. Although no particular relative reactivities are required to address the first issue, the chemistry that is involved at coupled sites must be similar enough to exhibit cross reactivities to observe autocatalysis. Autocatalysis then simply results when

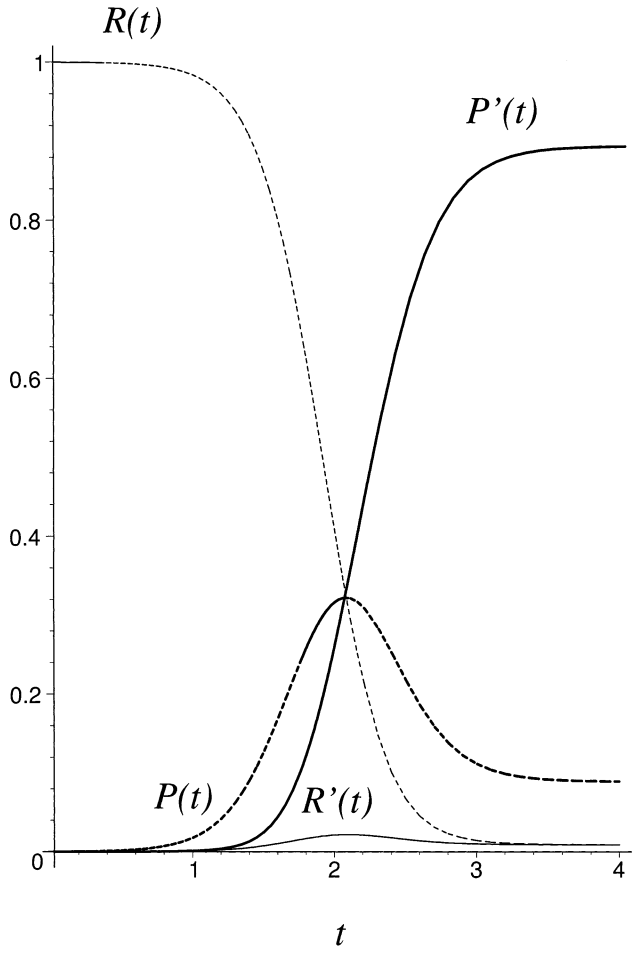

Figure 3. Autocatalysis in the case of a cross behavior. Time evolution of the concentrations R(t) (dotted thin line), R′(t) (solid thin line), P(t) (dotted thick line), and P′(t) (solid thick line) have been deduced from the numerical integration of eqs 9−14 for $k_1 = 0.001$, $k_{-1} = 0.0001$, $k_{2P} = k_{2P'} = 10$, $k_{-2P} = 100$, $k_{-2P'} = 1000$, $k_3 = 100$, $k_{-3} = 1$, $k_{4R} = k_{4R'} = 100$, $k_{-4R} = 100$, and $k_{-4R'} = 10$. Initial conditions are R(t) = 1, R′(t) = P(t) = P′(t) = 0.

the product of the reaction that is affecting one site is involved as a reactant in the reaction that is affecting the other site.

2.3. Experimental Illustration: Photoisomerization of 2,2′-Azopyridine. The photoisomerization of 2,2′-azopyridine,[26] as a function of pH and illumination, was chosen to illustrate some of the features of the proposed model.[27] The ongoing processes closely obey the mechanism given by reactions 3−6 (Figure 4). Some properties of this system were already investigated during research on photoresponsive crown ethers.[28]

In relation to the present issue, one can first be concerned with engineering the amount of cis versus trans isomers in the steady state and the rates for cis/trans interconversion under the given conditions of illumination. The process of trans−cis photoisomerization of the azo bond then is conceived to be tuned by the process of protonation that occurs at one pyridine. R and R′ respectively correspond to the unprotonated (**T**) and protonated (**TH**$^+$) trans isomers of the azoderivative, whereas P and P′ respectively designate the corresponding unprotonated (**C**) and protonated (**CH**$^+$) cis species. M identifies to the proton, whereas M′ does not appear in the kinetic scheme; pH alone is used for tuning. Conversely, one can also envisage the engineering of the relative amount of protonated species in the steady state and the rates for protonation/deprotonation reactions at a given pH. The process of protonation of one pyridine then is envisaged to be controlled by the photoisomerization process.

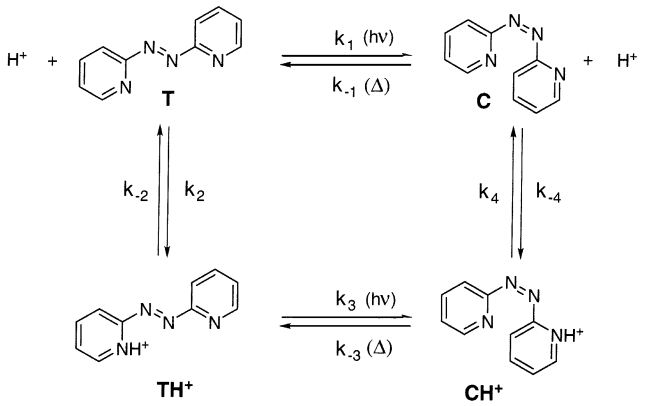

Figure 4. Schematic depiction of the pH-dependent photoisomerization of 2,2′-azopyridine as an experimental system to evaluate the present model.

R and R′ now correspond to the reactant states $\mathbf{H}^+ + \mathbf{T}$ and $\mathbf{H}^+ + \mathbf{C}$, respectively, whereas P and P′ now designate the $\mathbf{TH}^+$ and $\mathbf{CH}^+$ protonated species, respectively. M and M′ do not appear explicitly in the kinetic scheme anymore. In contrast, M is replaced by the tunable intensity I_0 of the illumination source in the reactions that describe the system evolution (see Supporting Information). The experiments were directed to evaluate all the relevant thermodynamic and rate constants involved in Figure 4.

The details for deriving the rate constants associated with the photo and thermal isomerizations from photoirradiation experiments are given in the Experimental Section and in the Supporting Information. In brief, diluted buffered aqueous solutions of the trans stereoisomer of 2,2′-azopyridine were irradiated at different pH and at various light intensities, and their UV−Vis absorption spectra were recorded as a function of time. A typical evolution is displayed in Figure 5a. In relation to the formation of the cis stereoisomer, the absorbance associated with the $\pi-\pi^*$ transition of the azopyridine chromophore slowly decreases as a function of time. The steady state is attained after ∼30 min, under the present experimental conditions. The light then was turned off and the relaxation to the initial state, which was composed of a mixture of protonated and unprotonated trans stereoisomers, was investigated by UV−Vis absorption (Figure 5b). The corresponding data were analyzed to extract (i) the quantum yields $\phi_{T\rightarrow C}$ and $\phi_{TH^+\rightarrow CH^+}$ that are respectively associated with the trans-to-cis photoisomerization of the unprotonated and protonated forms of the trans stereoisomer of 2,2′-azopyridine; (ii) the rate constants $k_{C\rightarrow T}$ and $k_{CH^+\rightarrow TH^+}$ associated with the corresponding reverse thermal cis-to-trans isomerizations. Thus, the following information was determined:

(1) $\phi_{T\rightarrow C} = 0.04 \pm 0.01$ and $\phi_{TH^+\rightarrow CH^+} = 0.07 \pm 0.02$. Under the typical conditions of illumination used in the present study ($I_0(\lambda_{exc}) = (5.0 \pm 0.1) \times 10^{-9}$ einstein/s), the latter values give $k_1 = (2.6 \pm 0.3) \times 10^{-3}$ s^{-1} and $k_{-1} = (3.0 \pm 0.3) \times 10^{-5}$ s^{-1}.

(2) $k_3 = (5.5 \pm 0.1) \times 10^{-3}$ s^{-1} and $k_{-3} = (2.0 \pm 0.1) \times 10^{-3}$ s^{-1}.

The rate constants associated to the protonation processes of the trans and cis stereoisomers of 2,2′-azopyridine were not measured during this study. In relation to the present work, only orders of magnitude were sought to evaluate the regime of exchange either (i) between the states **T** and **TH**$^+$, and **C** and **CH**$^+$, as a function of pH at a given light intensity, or (ii) between the states **T** and **C**, and **TH**$^+$ and **CH**$^+$, as a function of the light intensity at a given pH. After the proton dissociation constants pK_a of the **TH**$^+$ and **CH**$^+$ species are known, it is

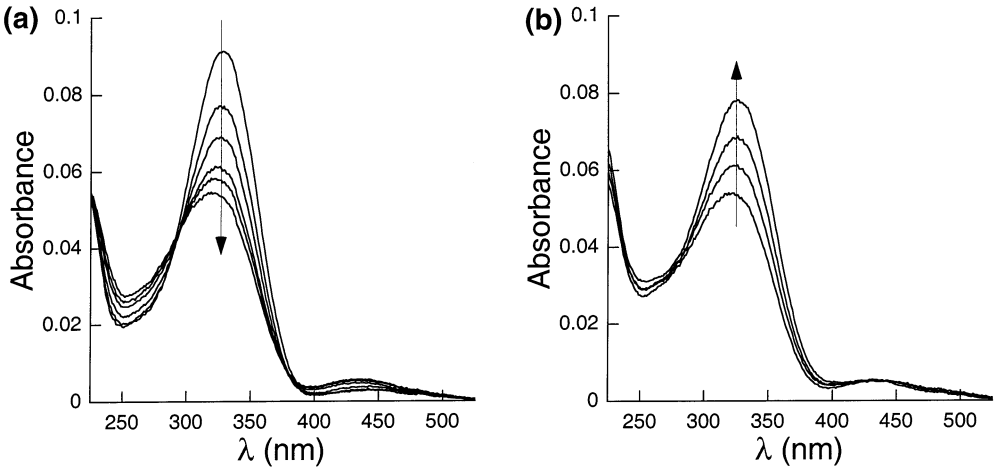

Figure 5. Temporal evolution of the absorbance of 2.5 mL of a solution initially containing $\mathbf{T} = T + TH^+$ at 6 μmol/L in the 0.1 mol/L buffer (pH = 2): (a) irradiation experiment data, showing UV−Vis absorption spectra recorded after 0, 2, 4, 8, 12, and 34 min of irradiation ($I_0(\lambda_{exc}) = 5 \times 10^{-9}$ einstein/s); and (b) relaxation experiment data, showing UV−Vis absorption spectra recorded after 0, 11, 29, and 59 min under the absence of irradiation.

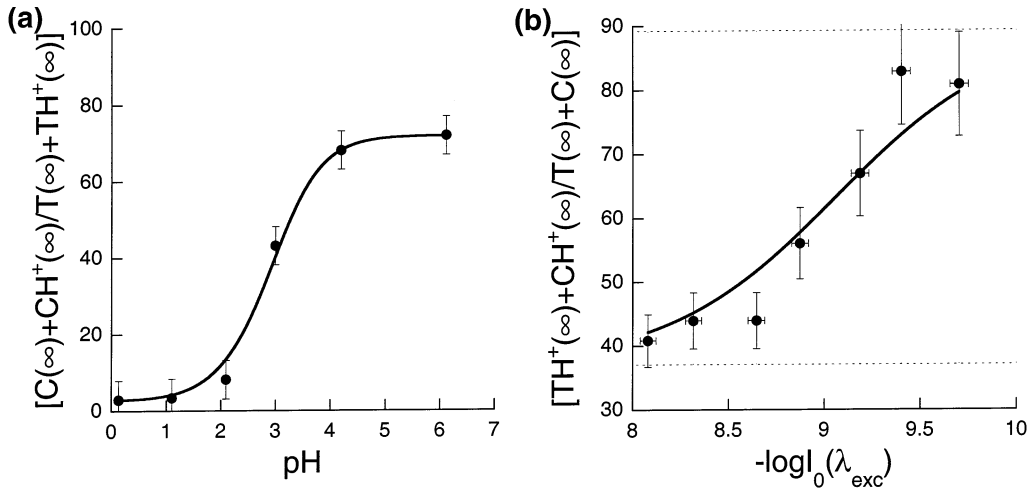

Figure 6. Experimental points and cuts (solid lines) of calculated surfaces $(C(\infty) + CH^+(\infty))/(T(\infty) + TH^+(\infty))$ and $(TH^+(\infty) + CH^+(\infty))/(T(\infty) + C(\infty))$. Panel a shows control of the process of trans−cis photoisomerization of the azo bond by the process of protonation occurring at one pyridine: $[(C(\infty) + CH^+(\infty))/(T(\infty) + TH^+(\infty))]$ vs pH for $I_0(\lambda_{exc}) = 5 \times 10^{-9}$ einstein/s. Panel b shows control of the process of protonation of one pyridine by the photoisomerization process: $[(TH^+(\infty) + CH^+(\infty))/(T(\infty) + C(\infty))]$ vs $-\log I_0(\lambda_{exc})$ at pH = 2. Dotted lines define asymptotic behavior derived from the pK_a values for $\mathbf{TH}^+$ and $\mathbf{CH}^+$.

possible to derive the dissociation rate constants of the protonated species, provided that the rate constants of protonation are available. In a first time, the proton dissociation constants for the trans ($K_a(\mathbf{TH}^+)$) and cis ($K_a(\mathbf{CH}^+)$) stereoisomers were measured (see panels a and b of Figure 4S, given in the Supporting Information). The former was extracted from the evolution of the UV−Vis absorption spectra of the trans stereoisomer, as a function of pH, whereas the latter was deduced from the fit of the rate constants associated with the cis-to-trans thermal isomerization, as a function of pH (see Experimental Section and Supporting Information). Proton dissociation constants of $pK_a(\mathbf{TH}^+) = 2.0 \pm 0.1$ and $pK_a(\mathbf{CH}^+) = 1.5 \pm 0.1$ were obtained. We then assumed that the rate of the protonation reaction of the pyridine ring in **T** and **C** was similar to that of pyridine alone. Such a hypothesis is reasonable upon consideration of the similar structure of the basic sites; no sterical hindrance or strong alteration of the solvation shell when going from the basic to the acidic form should make **T** and **C** singular, with regard to pyridine.[29−31] As a consequence, we adopted the reported pyridine value,[32] eventually leading to the following rate-constant values: $k_2 = k_{-4} \approx 10^{10}$ M^{-1} s^{-1}, $k_{-2} = k_2 10^{-pK_a(TH^+)} \approx (1.0 \pm 0.2) \times 10^8$ s^{-1} and $k_4 = k_{-4} 10^{-pK_a(CH^+)} \approx (3.1 \pm 0.6) \times 10^8$ s^{-1}.

After the latter experiments were performed, it became possible to analyze the dependence on pH and light intensity of the different features evoked in the preceding section, in relation to both properties: the amount of cis versus trans stereoisomers, or the amount of protonated versus unprotonated species of 2,2′-azopyridine in the steady state.

The ratios $(C(\infty) + CH^+(\infty))/(T(\infty) + TH^+(\infty))$ and $(TH^+(\infty) + CH^+(\infty))/(T(\infty) + C(\infty))$ are suitable variables to address the thermodynamic issues. In fact, the preceding series of experiments gave access to the steady-state concentrations in **T**, **C**, $\mathbf{TH}^+$, and $\mathbf{CH}^+$ under several investigated conditions of pH and light intensity $I_0(\lambda_{exc})$, so as to calculate the aforementioned ratios directly. In addition, the derivation of all the rate constants involved in the kinetic schemes displayed in Figure 4 allowed us to calculate $(C(\infty) + CH^+(\infty))/(T(\infty) + TH^+(\infty))$ and $(TH^+(\infty) + CH^+(\infty))/(T(\infty) + C(\infty))$ analytically, as a function of pH and $I_0(\lambda_{exc})$ (see the Supporting Information). Panels a and b in Figure 6 respectively display experimental points and cuts of the calculated surfaces either for a given value of

$I_0(\lambda_{exc})$ or at a given pH. Figure 6a shows that changing the pH value by 1 at pH ~3 determines the transition between two steady states that significantly differ in their compositions. Under the present conditions of illumination, one typically observes that ~30% of the trans stereoisomer remains for pH ≤1 ((C(∞) + CH^+(∞))/(T(∞) + TH^+(∞)) = 3), whereas only ~1% remains for pH ≥5 ((C(∞) + CH^+(∞))/(T(∞) + TH^+(∞)) = 60). In the present system, eqs 86 and 87 (given in Supporting Information) demonstrate that the corresponding compositions can be modified at will by changing the light intensity $I_0(\lambda_{exc})$ without changing the ratio between the two asymptotic values of (C(∞) + CH^+(∞))/(T(∞) + TH^+(∞)). Similarly, Figure 6b shows that changing the light intensity by 2 orders of magnitude is sufficient to go from one asymptotic steady state to the other. For large values of $I_0(\lambda_{exc})$, the cis stereoisomer dominates the behavior and the lower pK_a of the protonated cis species explains the resulting lower amount of protonated 2,2′-azopyridine in the steady state at a given pH. In contrast, the trans stereoisomer is predominant for low values of $I_0(\lambda_{exc})$. Correspondingly, more protonated 2,2′-azopyridine is observed in the steady state. Although changing the pH can affect the values of (TH^+(∞) + CH^+(∞))/(T(∞) + C(∞)) in both asymptotic regimes (see eqs 89 and 90 in the Supporting Information), their ratio is only determined by the intrinsic acid/base features of the cis and trans stereoisomers of 2,2′-azopyridine.

Kinetic considerations allow us to be certain if control over the chemical species by an auxiliary reaction makes sense for both types of situations evoked in the aforementioned discussion. Considering the range of investigated pH (0−7), the characteristic relaxation times associated with the protonation processes of the trans ($\tau_2 = [k_2 10^{-pH} + k_{-2}]^{-1}$) and cis ($\tau_4 = [k_{-4}10^{-pH} + k_4]^{-1}$) stereoisomers of 2,2′-azopyridine always remain inferior to 1 s. In contrast, the characteristic relaxation times associated to the photoisomerization processes of the unprotonated ($\tau_1 = [k_1 + k_{-1}]^{-1}$) and protonated ($\tau_3 = [k_3 + k_{-3}]^{-1}$) trans stereoisomers of 2,2′-azopyridine are always >1 min, under the irradiation conditions used during this study. Thus, the situation described in Figure 4 corresponds to tuning chemical species for the purpose of controlling the photoisomerization process via the protonation process. Indeed, **T** (or, correspondingly, **C**) and $\mathbf{TH}^+$ (or, correspondingly, $\mathbf{CH}^+$) are in a regime of fast exchange, with regard to photoisomerization. In contrast, reading Figure 4 vertically only reports the control over the relative proportions in cis and trans stereoisomers of 2,2′-azopyridine.

It is now possible to precisely evaluate the meaning of tuning the kinetic features that are associated with the photoisomerization process by altering the protonation process via pH. Under the present conditions of illumination, the longest relaxation time of the system may be continuously tuned between $\tau_1 = (1.3 \pm 0.1) \times 10^2$ s and $\tau_1 = (3.8 \pm 0.4) \times 10^2$ s upon changing the pH from 1 to 5. At the same time, the quantum yields for trans-to-cis isomerization of 2,2′-azopyridine will evolve from $\phi_{TH^+ \rightarrow CH^+} = 0.07 \pm 0.02$ to $\phi_{T \rightarrow C} = 0.04 \pm 0.01$, whereas the rate constants for thermal cis-to-trans isomerization will decrease from $k_{CH^+ \rightarrow TH^+} = (5.5 \pm 0.1) \times 10^{-3}$ s^{-1} to $k_{C \rightarrow T} = (3.0 \pm 0.3) \times 10^{-5}$ s^{-1}.

3. Two-Site Catalysis and Far-From-Equilibrium Conditions

3.1. The Model. We now wish to build a realistic kinetic mechanism that involves a two-site catalysis, which is nevertheless as simple as possible. In this goal, the following hypotheses are introduced. We consider a molecule E, typically an enzyme, that possesses two catalytic sites (denoted as 1 and 2). The reaction of interest—namely, the formation of product B from substrate A—is catalyzed by the first catalytic site, whereas the second site catalyzes the formation of B′ from A′. The concentration of the enzyme is supposed to be smaller than the concentration of the substrate. All the possible bimolecular reactions that involve the change of state of a given catalytic site are considered. In particular, all reverse reactions are considered. Trimolecular reactions, the change of state of two catalytic sites in a same step, and noncatalyzed reactions such as A ⇄ B are supposed to be highly unprobable, so that they can be neglected. Under these conditions, the mechanism, shown in Figure 7a, reads

$$\mathrm{A} + \mathrm{E} \underset{k_{-1}}{\overset{k_1}{\rightleftharpoons}} \mathrm{AE} \tag{18}$$

$$\mathrm{AE} + \mathrm{A}' \underset{k_{-2}}{\overset{k_2}{\rightleftharpoons}} \mathrm{AEA}' \tag{19}$$

$$\mathrm{AEA}' \underset{k_{-3}}{\overset{k_3}{\rightleftharpoons}} \mathrm{A} + \mathrm{EA}' \tag{20}$$

$$\mathrm{EA}' \underset{k_{-4}}{\overset{k_4}{\rightleftharpoons}} \mathrm{E} + \mathrm{A}' \tag{21}$$

$$\mathrm{AEA}' \underset{k_{-5}}{\overset{k_5}{\rightleftharpoons}} \mathrm{B} + \mathrm{EA}' \tag{22}$$

$$\mathrm{EA}' \underset{k_{-6}}{\overset{k_6}{\rightleftharpoons}} \mathrm{B}' + \mathrm{E} \tag{23}$$

$$\mathrm{B} + \mathrm{E} \underset{k_{-7}}{\overset{k_7}{\rightleftharpoons}} \mathrm{AE} \tag{24}$$

$$\mathrm{AE} + \mathrm{B}' \underset{k_{-8}}{\overset{k_8}{\rightleftharpoons}} \mathrm{AEA}' \tag{25}$$

The effect of a reaction can be viewed as a change of the state for one catalyst site, which is observed easier when the following notations are adopted: E = 1∅2∅, AE = 1*a*2∅, EA′ = 1∅2*a*′, and AEA′ = 1*a*2*a*′. The coupling between sites 1 and 2 implies that the reactivity of site 1 changes with the state of site 2. Consequently, the values of the rate constants k_1 and k_{-3}, k_{-1} and k_3, k_2 and k_{-4}, k_{-2} and k_4, k_5 and k_{-7}, k_{-5} and k_7, k_6 and k_{-8}, and k_{-6} and k_8 are generally different (see section 4). At chemical equilibrium, a detailed balance imposes relations between the thermodynamic constants $K_i = k_i/k_{-i}$. They are obtained by requiring that the rate of each step is equal to the rate of the corresponding inverse process. This relation is expressed as follows:

$$K_1 K_3 = K_5 K_7 = K_{-2} K_{-4} = K_{-6} K_{-8} \tag{26}$$

The idea is to exert constraints on the second site of the catalyst, to induce a certain amount of control of the properties of the first site and, in particular, to modify its reactivity and catalytic efficiency. We choose to introduce reservoirs of substrate A′ and product B′ for maintaining constant concentrations of A′ and B′ in the system. Fixing the concentrations of A′ and B′ is sufficient here to maintain the system out of chemical equilibrium if the condition

$$\frac{\mathrm{B}'}{\mathrm{A}'} \neq \left(\frac{\mathrm{B}'}{\mathrm{A}'}\right)_{eq} = K_2 K_{-8} \tag{27}$$

is fulfilled. As shown in Figure 7b, the four reactions that appear in Figure 7a (reactions 2, 4, 6, and 8) can be rewritten in the

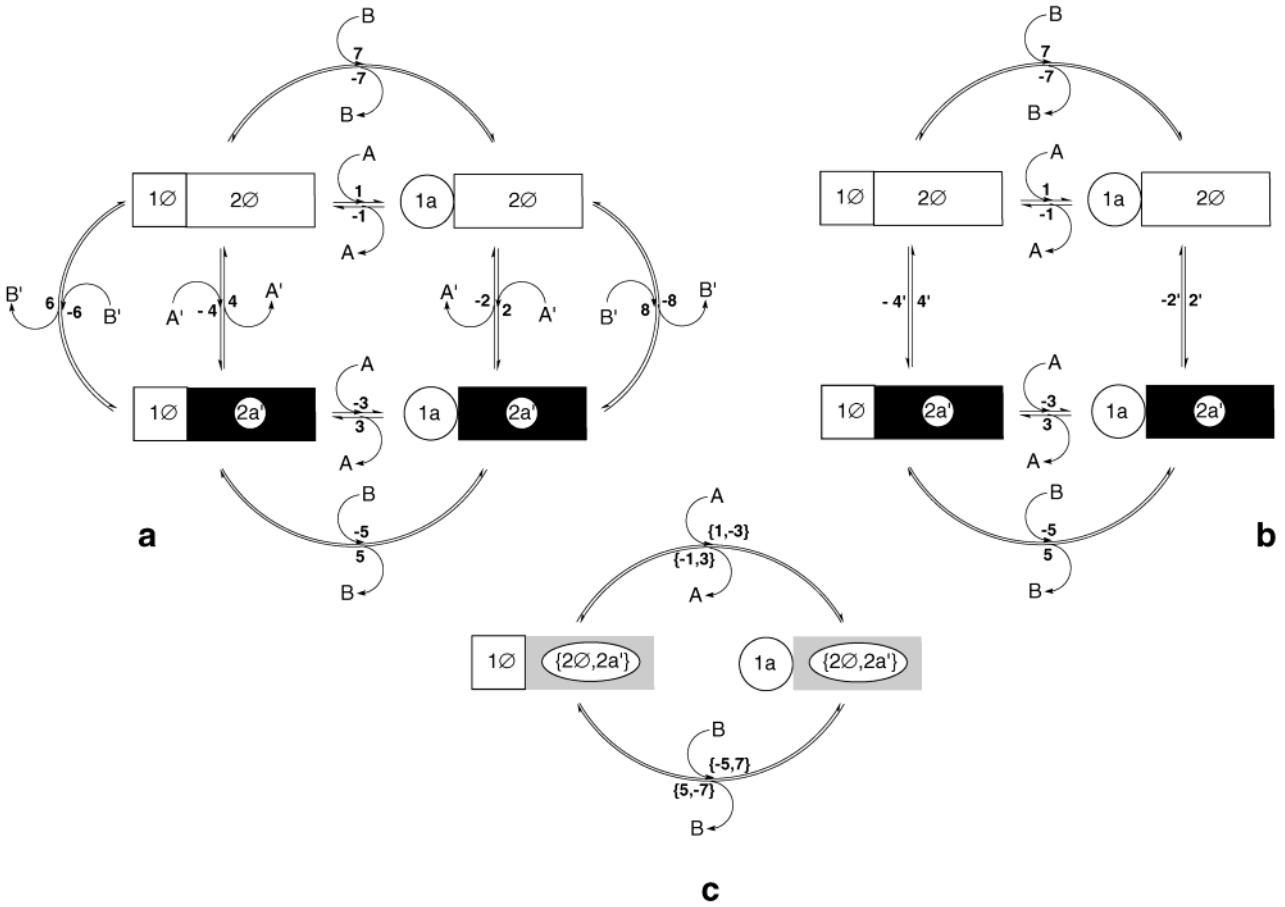

Figure 7. Schematic depiction of the mechanism involved in two-site catalysis and far-from-equilibrium conditions: (a) general form, (b) reduced form for concentrations of A′ and B′ maintained constant, and (c) reduced form for concentrations of A′ and B′ maintained constant and for {E, EA′} and{AE, AEA′} ≡ A{E, EA′} in a regime of fast exchange. Legend: E = 1∅2∅, AE = 1*a*2∅, EA′ = 1∅2*a*′, and AEA′ = 1*a*2*a*′.

following equivalent, more-compact, form:

$$\mathrm{AE} \underset{k'_{-2}}{\overset{k'_2}{\rightleftharpoons}} \mathrm{AEA'} \tag{28}$$

$$\mathrm{EA'} \underset{k'_{-4}}{\overset{k'_4}{\rightleftharpoons}} \mathrm{E} \tag{29}$$

where the rate constants of the reduced mechanism obey the relations

$$\begin{aligned} k'_2 &= k_2\mathrm{A'} + k_8\mathrm{B'} \\ k'_{-2} &= k_{-2} + k_{-8} \\ k'_4 &= k_4 + k_6 \\ k'_{-4} &= k_{-4}\mathrm{A'} + k_{-6}\mathrm{B'} \end{aligned} \tag{30}$$

Because of their dependence on the concentrations of A′ and B′, the rate constants k'_2 and k'_{-4} will be called controlled rate constants, instead of actual rate constants. When the concentrations of A′ and B′ are fixed by external constraints, the mechanism reduces to the six steps given in eqs 18, 20, 22, 24, 28, and 29. Note that a detailed balance is violated in this out-of-equilibrium system. In particular, we choose concentrations values for A′ and B′ such that

$$K'_2K'_4 \neq K_2K_4 \tag{31}$$

where $K'_i = k'_i/k'_{-i}$. Taking into consideration the two conservation laws that were deduced from the conservation of substrate-derived and enzyme-derived species, the evolution of the six variable concentrations (A, B, E, AE, AEA′, and EA′) is governed by four differential equations (see Supporting Information).

In the present section, diverse behaviors of this dynamical system are explored, depending on the values of the rate constants and the concentrations of A′ and B′, which are fixed by the reservoirs. It will be shown that such a minimal system can be used to tune reaction yields. The corresponding result bears some significance for free-energy transduction and, as such, for transferring out-of-equilibrium conditions in a chemical system.[33] We also wish to illustrate that, for well-chosen values of the parameters, the kinetic scheme involves an autocatalytic step. Eventually, it will be shown that the model possesses enough ingredients to reproduce the so-called phenomenon of kinetic proofreading:[34,35] the system is able to discriminate between reactants that differ by some rate-constant values in proportions that are much better than those predicted by equilibrium thermodynamics.

3.2. Theoretical Predictions. *3.2.1. Tuning Reaction Yield.* In this section, we are interested in stationary solutions. The reaction yield is defined as the reaction quotient $(\mathrm{B}/\mathrm{A})_\infty$ that is attained when the system is in a steady state. If the system is isolated, the reaction quotient that is attained asymptotically is given by the equilibrium constant of the net reaction A ⇌ B and reduces to

$$\left(\frac{\mathrm{B}}{\mathrm{A}}\right)_{\mathrm{eq}} = K_1K_{-7} \tag{32}$$

Our goal is to show that exchanges with the exterior fixing A′

and B′ to appropriate values can force the reaction quotient to be different from $(B/A)_{eq}$.

In the spirit of forcing using an auxiliary reaction, and to find an explicit analytical expression for the reaction quotient, we admit that reactions 28 and 29 reach a partial equilibrium state before the other reactions. The hypothesis consists of assuming that reactions 28 and 29 are fast, and the hypothesis is as follows:

$$E \approx \left(\frac{k'_4}{k'_{-4}}\right) EA' \qquad AEA' \approx \left(\frac{k'_2}{k'_{-2}}\right) AE \tag{33}$$

Under this condition, the kinetic mechanism may be reduced, as shown in Figure 7c. Using eq 33 in this paper and eqs 93 and 95 that are given in the Supporting Information, the scaled reaction yield obeys the following relation (see Supporting Information):

$$\rho(K'_2, K'_4) = \frac{(B/A)_\infty}{(B/A)_{eq}} = \frac{[1 + (k_5/k_{-7})K'_2][K'_4 + (k_{-3}/k_1)]}{[1 + (k_3/k_{-1})K'_2][K'_4 + (k_{-5}/k_7)]} \tag{34}$$

Departures of $\rho(K'_2, K'_4)$ from a value of 1 make the possibilities of tuning that are offered by nonequilibrium conditions explicit. The most interesting behaviors are observed when K'_2 and K'_4 are simultaneously either very large or very small. The two limit values that are attained obey $\rho(\infty,\infty) = 1/\rho(0,0)$. Note that the asymptotic value given in eq 34 is not a detailed balance solution. Each reactive process is not compensated by the realization of the inverse process such as that at equilibrium. The consumption of species A′ or B′ by a given reaction is instantaneously compensated by an appropriate exchange with the reservoir of this species. The variations of the scaled reaction yield, which is considered to be a function of the concentration of A′ and B′ and is deduced from eqs 30 and 34, are given in Figure 8. Two different situations are illustrated in Figure 8a and b for the same set of rate constants for reactions 1, 3, 5, and 7. In Figure 8a, the difference $(k_2/k_{-4}) - (k_8/k_{-6})$ is relatively small and the extrema do not reach the limit values $\rho(0,0)$ and $\rho(\infty,\infty)$. Figure 8b displays the scaled reaction yield for an enlarged $(k_2/k_{-4}) - (k_8/k_{-6})$ difference. A plateau reaching $\rho(0,0)$ and $\rho(\infty,\infty)$ can now be observed.

The preceding results prove that using a two-site catalyst and imposing appropriate exchanges of matter allow us to choose the value of the reaction quotient $(B/A)_\infty$ in the steady state. The limits of tuning rely on two independent sets of rate constants: $\{k_{-1}, k_3, k_5, k_{-7}\}$, to fix $\rho(\infty,\infty)$, and $\{k_2, k_{-4}, k_{-6}, k_8\}$, to determine which part of the A′, B′ space is actually explored. The achievement of a large range for the variation of the reaction yield will be dependent on the quality of the design of the two-site catalyst. In fact, the ratios k_{-1}/k_3, k_5/k_{-7}, k_2/k_{-4}, and k_8/k_{-6} will be dependent on the nature of the coupling between both sites. For instance, the enhancement of $\rho(\infty,\infty)$ can be achieved if the presence of A′ on the second site of the catalyst makes the unbinding of A on site 1 more difficult and the unbinding of B from site 1 easier (a large value of the product $(k_{-1}/k_3) \times (k_5/k_{-7})$). Simultaneously, having a large difference between k_2/k_{-4} and k_8/k_{-6} implies that the presence of A on site 1 now has an impact on the arrival of A′ on site 2 that is different from the effect that it has on the arrival of B′.

3.2.2. Autocatalysis. We are now interested in a kinetic property and consider the differential equations for the concentrations of species that obey the mechanism given in eqs 18−25 (see Supporting Information). We look for an autocatalytic step such that the formation rate of a species is proportional to its own concentration, possibly after the elimination of fast variables. When following the time evolution of the concentration of an autocatalytic species, one observes a typical sigmoidal curve, which characterizes a long induction period, followed by a sudden increase toward the final stationary state. In fact, such explosive behavior can be observed in the case of the mechanism that is given in eqs 18−25, as shown in Figure 9 for well-chosen rate-constant values. The results were obtained by numerically integrating the exact differential equations, using the Euler method. In the case of a one-site catalyst, the model

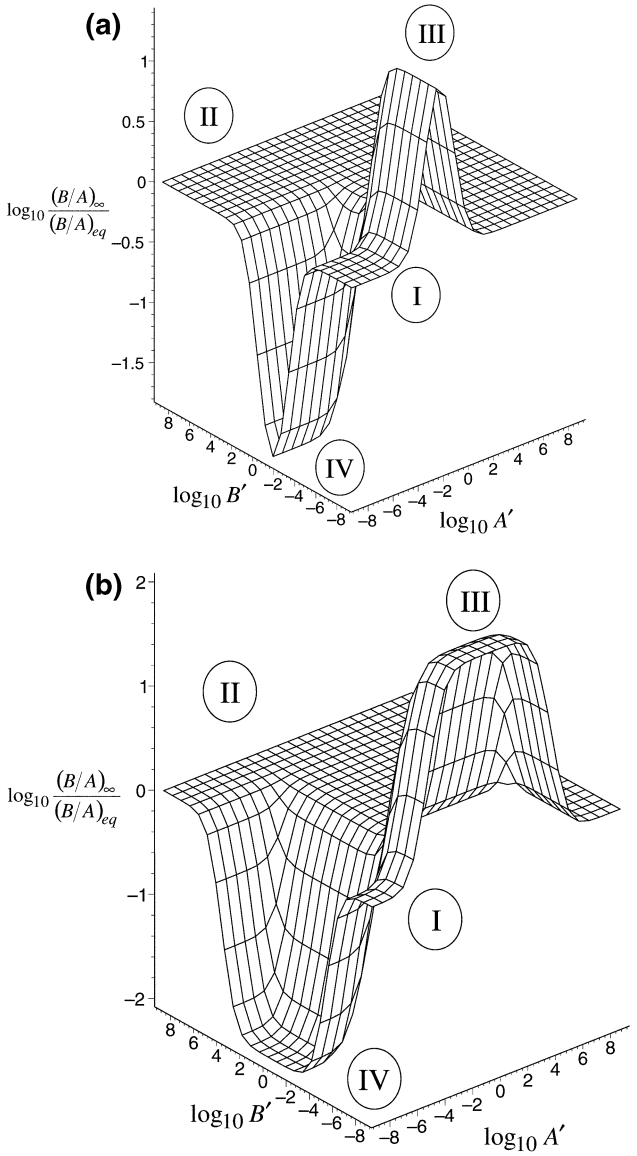

Figure 8. Three-dimensional plots that illustrate the tuning reaction yield. Logarithmic plots of the scaled reaction quotient $(B/A)_\infty/(B/A)_{eq}$ versus control parameters A′ and B′ are shown for the following rate-constant values: (a) $k_1 = 0.1$, $k_{-1} = 100$, $k_2 = 100$, $k_{-2} = 1$, $k_3 = 100$, $k_{-3} = 10$, $k_4 = 1$, $k_{-4} = 1$, $k_5 = 10$, $k_{-5} = 1$, $k_6 = 100$, $k_{-6} = 100$, $k_7 = 0.0001$, $k_{-7} = 0.1$, $k_8 = 0.1$, $k_{-8} = 0.001$; (b) $k_1 = 0.1$, $k_{-1} = 100$, $k_2 = 10^4$, $k_{-2} = 1$, $k_3 = 100$, $k_{-3} = 10$, $k_4 = 10^{-5}$, $k_{-4} = 10^{-3}$, $k_5 = 10$, $k_{-5} = 1$, $k_6 = 10^4$, $k_{-6} = 0.1$, $k_7 = 0.0001$, $k_{-7} = 0.1$, $k_8 = 10^{-5}$, and $k_{-8} = 0.1$. The regions labeled I, II, III, and IV, respectively, correspond to K'_2 small and K'_4 large, K'_2 large and K'_4 small, K'_2 and K'_4 large, and K'_2 and K'_4 small.

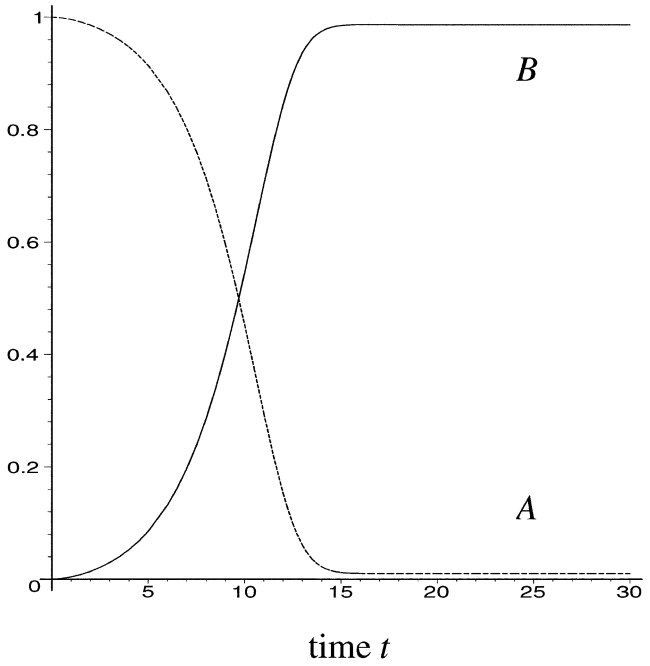

Figure 9. Autocatalytic behavior involved in two-site catalysis and far-from-equilibrium conditions. Time evolution of the concentrations of species A and B have been deduced from the numerical integration of eqs 93−96 in the Supporting Information for $k_1 = 0.001$, $k_{-1} = 0.001$, $k_2 = 10$, $k_{-2} = 1$, $k_3 = 10$, $k_{-3} = 100$, $k_4 = 0.001$, $k_{-4} = 0.001$, $k_5 = 100$, $k_{-5} = 10$, $k_6 = 0.01$, $k_{-6} = 0.001$, $k_7 = 1$, $k_{-7} = 100$, $k_8 = 1$, $k_{-8} = 1$, $A_0 = 1$, $E_0 = 0.1$, $A' = 1$, and $B' = 1$.

reduces to the standard Michaelis−Menten mechanism, A + E ⇌ AE ⇌ B + E, and does not present any autocatalytic behavior.

Thus, two-site catalysts seem to be an alternative to the procedure evoked in the previous section toward the design of simple organic autocatalytic systems. In fact, the present behavior is reminiscent of some features of the phosphofructokinase that is involved in glycolytic oscillations.[3] This enzyme is comprised of multiple subunits that carry catalytic sites that are specific for the substrate and regulatory sites on which activators bind and, thereby, tune the enzyme activity.

3.2.3. Kinetic Proofreading. Finally, we wish to show that the introduction of a second site on a catalyst is a simple way to decrease the percentage of incorrect reactant matches. In other words, our goal is now to exhibit appropriate rate-constant values, such that the kinetic scheme introduced in eqs 18, 20, 22, 24, 28, and 29 possesses the property of kinetic proofreading. Hopfield[34] and Ninio[35] introduced this concept to explain how biological processes may achieve error rates below those expected on the basis of equilibrium thermodynamics.[36,37] Starting from the Michaelis−Menten mechanism, Hopfield showed that repeating a recognition step, i.e., requiring a second intermediate species produced by an irreversible step, significantly reduces the transformation rate of incorrect reactants A^i, which are supposed to differ from the correct reactant A by smaller values of two rate constants.

Considering a set of coupled nonlinear kinetic equations, such as those associated with eqs 18, 20, 22, 24, 28, and 29, we use a general method to find stationary solutions with predefined properties. Orders of magnitude are assigned to the rate constants and to the steady-state concentrations of each species, to extract solutions from the corresponding differential equations. If a solution is found at leading order, it possesses a priori the desired features. The rate constants of reactions that concern the incorrect species A^i here are supposed to be the same as those of A, except for $k^i_{-1} > k_{-1}$ and $k^i_3 > k_3$. At equilibrium, the percentage of incorrect matching of reagents obeys the relation[34]

$$\left(\frac{B^i}{B}\right)_{eq} \sim \frac{k_{-1}}{k^i_{-1}} \tag{35}$$

Here, we impose

$$k_1 \approx 1,\ k_{-1} \approx \frac{1}{\epsilon},\ k^i_{-1} \approx \frac{1}{\epsilon^2},\ k'_2 \approx 1,\ k'_{-2} \approx 1 \tag{36}$$

$$k_3 \approx \frac{1}{\epsilon},\ k^i_3 \approx \frac{1}{\epsilon^2},\ k_{-3} \approx \epsilon^2,\ k'_4 \approx 1,\ k'_{-4} \approx 1 \tag{37}$$

$$k_5 \approx \epsilon,\ k_{-5} \approx \epsilon,\ k_7 \approx \epsilon,\ k_{-7} \approx \epsilon^3 \tag{38}$$

where ϵ is small, and search for a solution that obeys the relations

$$A \approx 1,\ B \approx \epsilon^2,\ E \approx 1,\ AE \approx \epsilon,\ AEA' \approx \epsilon^2,\ EA' \approx 1 \tag{39}$$

We do not claim that this choice is unique. In fact, a sensitivity analysis of the dynamical system to the various parameters would be necessary to check the robustness of the behavior. In the present set, note the severe conditions that are imposed on k_{-7} to prevent the direct formation of B without going through the second intermediate AEA′. At leading order in ϵ, the reaction yield obeys the relation

$$\left(\frac{B}{A}\right)_\infty \approx \frac{k_1 k'_2 k'_4 k_5}{k_{-1} k_3 k'_{-4} k_{-5}} \tag{40}$$

The goal here is not to optimize the reaction yield, which scales as ϵ^2. The important point is that the ratio $(B/A)_\infty$ is inversely proportional to the product of the two rate constants k_{-1} and k_3, which differ when comparing correct and incorrect reagents. Consequently, the error fraction $(B^i/B)_\infty$ that characterizes the percentage of incorrect matching of reagent scales at the leading order as

$$\left(\frac{B^i}{B}\right)_\infty \approx \frac{k_{-1} k_3}{k^i_{-1} k^i_3} \tag{41}$$

Taking into account the relation $k_3/k_{-1} = k^i_3/k^i_{-1}$ that is imposed by a detailed balance, we find that the error fraction scales as the square of its equilibrium prediction that is recalled in eq 35.

This result shows that our kinetic scheme, which involves a two-site catalysis and the use of two reservoirs, possesses the property of kinetic proofreading when the orders of magnitude of the rate constants are appropriate. The present approximate analytical predictions are confirmed by the determination of the stationary error fraction for numerical values of the rate constants that obey the scaling relations given in eqs 36−39 with $\epsilon = 0.1$. The variation of the error fraction with the two controlled concentrations {A′, B′} is given in Figure 10. There is a domain in parameter space, {A′, B′}, where k'_{-2} and k'_{-4} obey the scaling law that is given in eqs 36 and 37 and where the error fraction tends to the square of its equilibrium prediction. Note that, contrary to what could be believed when considering the name of kinetic proofreading, this phenomenon characterizes a property of the steady state that is attained by the system.

4. Discussion

To make precise the potential of the present approach, different types of coupling between molecular sites are exam-

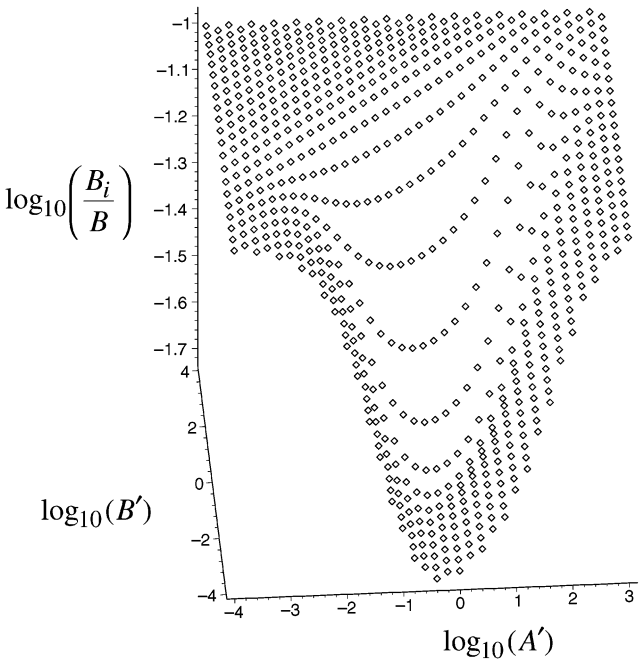

Figure 10. Kinetic proofreading emerging from two-site catalysis and far-from-equilibrium conditions. A logarithmic plot of the error fraction B_i/B versus control parameters A′ and B′ is shown for the following rate-constant values: $k_1 = 1$, $k_{-1} = 10$, $k^i_{-1} = 100$, $k_2 = 1$, $k_{-2} = 0.5$, $k_3 = 10$, $k^i_3 = 100$, $k_{-3} = 0.01$, $k_4 = 0.0005$, $k_{-4} = 0.1$, $k_5 = 1$, $k_{-5} = 1$, $k_6 = 1$, $k_{-6} = 1$, $k_7 = 0.1$, $k_{-7} = 0.001$, $k_8 = 0.005$, and $k_{-8} = 0.5$.

ined. In a small molecule, coupling can result from through-space interactions, such as electrostatic interaction, when both coupled sites involve charged species. For instance, the appearance of a charge following protonation at a given site may affect some further reactivity that occurs at another site because of the changes of energy barriers that are linked to electrostatic effects.[38] Coupling can also result from through-bond interactions that induce changes of bond polarity or conformational rearrangements. The two types of interaction probably operate in the case of the investigated example where the protonation of a pyridine N atom alters the cis/trans isomerization of 2,2′-azopyridine. All these types of coupling involve perturbations whose energies are typically associated with intermolecular interactions. Thus, one anticipates the difference of the standard Gibbs free energies $|\Delta_1 G° - \Delta_3 G°|$ to lie within a range of a few *RT*, where $\Delta_1 G°$ and $\Delta_3 G°$ are associated with reactions 3 and 5, respectively. Upon consideration of the relation

$$\frac{K_1}{K_3} = \exp\left(-\frac{\Delta_1 G° - \Delta_3 G°}{RT}\right) \qquad (42)$$

up to 3 orders of magnitude could be typically observed between the values of K_1 and K_3 for a small molecule. Indeed, one observes in the present experimental system that $K_1/K_3 = 3 \times 10^1$, which lies within the expected range. In fact, all the values of the rate constants that were used throughout this paper for illustration fulfill the latter orders of magnitude making it possible to design artificial systems that would exhibit the present complex behaviors. In relation to future attempts to design microscopic structures, attention should be given to the fact that through-space and through-bond types of coupling are generally short range (<1 nm); thus, such an approach seems especially suitable when polycondensations between small monomeric units are used to synthesize the reactant R. One can, nevertheless, imagine much longer ranges to become accessible as soon as more-sophisticated structures, such as fused cycles,[39] or rigid secondary structures, such as those in proteins, are involved.

5. Conclusion

This paper examines a simple strategy that relies on a general frame to engineer several aspects of complexity in chemical systems. The deliberate introduction of an auxiliary reactive site on a substrate and the appropriate choice of external constraints is suggested as a powerful way to observe a rich collection of dynamic and asymptotic behaviors. As experimentally illustrated by the pH-dependent photoisomerization of *trans*-2,2′-azopyridine, such an approach can be used for local and continuous tuning of the yield and the rate constants of a reaction of interest. In relation to the present purpose, this step is significant, because the more-elaborated behaviors that have been reported often rely on appropriate scaling of the rate constants. Indeed, some promising features offered by far-from-equilibrium conditions have been analyzed. In the case of a two-site catalysis, it was shown that a reaction yield can be tuned at will in the steady state, independent of the constraints that are imposed by a detailed balance at equilibrium. It was also proved that a two-site catalysis may reproduce kinetic proofreading, i.e., a percentage of mismatch of reactants, that is much smaller than that near equilibrium. In addition, autocatalysis can be observed in a two-site catalysis, which offers an alternative to the cross behavior between two-site reactants and products.

6. Experimental Section

6.1. Synthesis. *6.1.1. Trans 2,2′-Azopyridine, **T**.* 2-Aminopyridine (941 mg, 10 mmol) and activated manganese dioxide (22 g, 250 mmol) were heated in benzene (60 mL) for 6 h;[40] water was extracted using a Dean Stark apparatus. After the mixture was cooled, the resulting suspension was filtered and the filtrate was evaporated. The crude product was purified by recrystallization to yield 870 mg (94%) of red crystals of the trans stereoisomer of 2,2′-azopyridine **T**: mp 85 °C (cyclohexane, lit.[26] 85−86 °C, petroleum ether); ^{1}H NMR (250 MHz, $CDCl_3$): $\delta = 8.85-8.75$ (m, 2H), 8.10−7.90 (m, 4H), 7.55−7.45 (m, 2H); ^{1}H NMR (400 MHz, D_2O): $\delta = 8.62$ (ddd, $J_{H_3H_4} = 4.8$ Hz, $J_{H_3H_5} = 1.8$ Hz, $J_{H_3H_6} = 0.8$ Hz, $2H_3$), 8.11 (td, $J_{H_5H_6} = J_{H_5H_4} = 7.8$ Hz, $J_{H_5H_3} = 1.8$ Hz, $2H_5$), 7.95 (dt, $J_{H_6H_5} = 8.0$ Hz, $J_{H_6H_3} = J_{H_6H_4} = 0.8$ Hz, $2H_6$) 7.62 (ddd, $J_{H_4H_5} = 7.6$ Hz, $J_{H_4H_3} = 4.8$ Hz, $J_{H_4H_6} = 1.1$ Hz, $2H_4$).

*6.1.2. Determination of the Photoproduct from Isomerization of **T** in Aqueous Solutions.* A quantity (1.5 mL) of 4.2×10^{-3}-mol/L **T** in D_2O (pH = 6.8) was irradiated with a light intensity of $I_0(328) = 5 \times 10^{-9}$ einstein/s. ^{1}H NMR (400 MHz, D_2O) unambiguously demonstrated that the system only contained a 35:65 (mol/mol) mixture of trans:cis stereoisomers of 2,2′-azopyridine in the steady state. ^{1}H NMR (400 MHz, D_2O) of **C**: $\delta = 8.17$ (d, $J_{H_3H_4} = 4.4$ Hz, $2H_3$), 7.89 (td, $J_{H_5H_6} = J_{H_5H_4} = 7.8$ Hz, $J_{H_5H_3} = 1.7$ Hz, $2H_5$), 7.29 (dd, $J_{H_4H_5} = 7.6$ Hz, $J_{H_4H_3} = 4.9$ Hz, $2H_4$), 7.25 (d, $J_{H_6H_5} = 8.0$ Hz, $2H_6$).

6.2. UV/Vis Spectroscopic Measurements. The UV−Vis absorption spectra were recorded on a Kontron model Uvikon-940 spectrophotometer at 293 K.

6.2.1. Irradiation Experiments. All experiments were performed at 293 K in Britton−Robinson buffers at a concentration of 0.1 mol/L, prepared according to the work by Frugoni.[41] Irradiations were made at wavelengths of 320−330 nm on 2.5 mL samples in 1 cm × 1 cm quartz fluorescence cuvettes under constant stirring. The absorbances of the samples at the excitation wavelength were <0.1 during all the irradiation

experiments. Excitations were performed with the 75 W xenon lamp of a Photon Technology International model LPS 220 spectrofluorometer at several slit widths. The corresponding incident light intensities were calibrated by determining the kinetics of photoconversion of the α-(*p*-dimethylaminophenyl)-*N*-phenylnitrone to 3-(*p*-dimethylaminophenyl)-2-phenyloxaziridine in fresh dioxane.[42] Each light intensity $I_0(\lambda_{exc})$ was extracted from the corresponding experimental kinetic constant (k_{ref}) by means of linear regression of the logarithmic plot of the absorbance at 380 nm upon excitation at $\lambda_{exc} = 320$ nm, using

$$I_0(\lambda_{exc}) = \frac{k_{ref}A_{tot}(\lambda_{exc})V}{\epsilon_N(\lambda_{exc})\phi[1 - \exp(-2.3A_{tot}(\lambda_{exc}))]} \quad (43)$$

where $A_{tot}(\lambda_{exc})$ is the total absorbance at the excitation wavelength (which remains essentially constant during the illumination experiment), V the volume of the irradiated sample, and $\epsilon_N(\lambda_{exc})$ the molar absorption coefficient of the nitrone at the excitation wavelength. The parameter ϕ is taken to be equal to 0.21.[42]

6.2.2. Determination of the Relaxation Time τ of the Irradiated Sample. The temporal evolution of the total absorbance $A_{tot}(\lambda_{obs})$ of the sample was fitted according to eq 81 (see Supporting Information) to extract the α parameter that is defined in eq 78 in the Supporting Information, which is the inverse of the relaxation time τ of the system. (See Figure 2Sa in the Supporting Information for an illustration at pH = 2.)

6.2.3. Determination of the Rate Constants Associated with the Thermal Process of Cis-to-Trans Isomerization. After the photostationary state was attained during the irradiation experiment, the sample was removed from the excitation beam and transferred to a dark chamber. The evolution of its total absorbance at the maximum of absorption of the trans stereoisomer $A_{tot}(\lambda_{max})$ then was recorded, as a function of time, to extract $k_{C\rightarrow T}$ from the data fit according to eq 83 in the Supporting Information. (See Figure 2Sb in the Supporting Information for an illustration at pH = 2.)

6.2.4. Determination of Proton Dissociation Constants. A titration of a **T** solution by a concentrated HCl solution was performed to derive $pK_a(\mathbf{TH}^+)$ of the protonated *trans*-2,2′-azopyridine. The fit of the curve $A_{tot}(\lambda_{TH^+})/A_{tot}(\lambda_T)$, where λ_{TH^+} and λ_T respectively designate the maximum absorption wavelengths of $\mathbf{TH}^+$ and **T**, according to

$$\frac{A_{tot}(\lambda_{TH^+})}{A_{tot}(\lambda_T)} = \frac{\epsilon_{TH^+}(\lambda_{TH^+})10^{-pH} + \epsilon_T(\lambda_{TH^+})K_a(TH^+)}{\epsilon_{TH^+}(\lambda_T)10^{-pH} + \epsilon_T(\lambda_T)K_a(T)} \quad (44)$$

yielded $pK_a(\mathbf{TH}^+) = 2.0 \pm 0.1$ (see Figure 4Sa in the Supporting Information). The same experiment provided the molar absorption coefficients of **T** and $\mathbf{TH}^+$ in the investigated range of wavelengths (see Figure 4Sa). The value of $pK_a(\mathbf{CH}^+)$ of the protonated *cis*-2,2′-azopyridine was derived from fitting the curve $k_{C\rightarrow T}$ as a function of pH, according to eq 73 in the Supporting Information, to obtain $pK_a(\mathbf{CH}^+) = 1.5 \pm 0.1$ (see Figure 4Sb in the Supporting Information). In addition, one obtained $k_{C\rightarrow T} = (3.0 \pm 0.3) \times 10^{-5}\ s^{-1}$ and $k_{CH^+\rightarrow TH^+} = (2.0 \pm 0.1) \times 10^{-3}\ s^{-1}$ from the same fits. The present values satisfactorily compare with reported values that were obtained under slightly different experimental conditions.[28]

6.2.5. Derivation of the System Composition in the Photostationary State under Illumination. The percentage of the trans isomer $\mathbf{T}(\infty)$ in the photostationary state at any pH was deduced from the measurements of α and $k_{C\rightarrow T}$ by applying eq 82 from the Supporting Information. From the latter result and from the $pK_a(\mathbf{TH}^+)$ value that was determined during the preceding series of experiments, it was possible to determine the molar absorption coefficients of **C** and $\mathbf{CH}^+$ in the investigated range of wavelengths (see Figure 3Sb in the Supporting Information).

6.2.6. Derivation of the Final Rate Constants. The values of α and $k_{C\rightarrow T}$ at any pH were used to extract $k_{T\rightarrow C}$ using eq 78 from the Supporting Information. Eventually, the desired rate constants related to the cis-to-trans isomerization processes were obtained from the asymptotic values obtained at low and high pH resulting from the fits according to eqs 72 and 73 (see Figure 4Sb). Thus, one obtains the relations

$$k_{TH^+\rightarrow CH^+} = \frac{2.3\epsilon_{TH^+}(\lambda_{exc})\phi_{TH^+\rightarrow CH^+}I_0(\lambda_{exc})}{V} = (5 \pm 1) \times 10^{-3}\ s^{-1} \quad (45)$$

$$k_{T\rightarrow C} = \frac{2.3\epsilon_T(\lambda_{exc})\phi_{T\rightarrow C}I_0(\lambda_{exc})}{V} = (3 \pm 1) \times 10^{-3}\ s^{-1} \quad (46)$$

$$\phi_{TH^+\rightarrow CH^+} = (7 \pm 2) \times 10^{-2} \quad (47)$$

$$\phi_{T\rightarrow C} = (4 \pm 1) \times 10^{-2} \quad (48)$$

and, in relation to Figure 4,

$$k_1 = \frac{2.3\epsilon_T(\lambda_{exc})\phi_{T\rightarrow C}I_0(\lambda_{exc})}{V} \quad (49)$$

$$k_{-1} = k_{C\rightarrow T} \quad (50)$$

$$k_3 = \frac{2.3\epsilon_{TH^+}(\lambda_{exc})\phi_{TH^+\rightarrow CH^+}I_0(\lambda_{exc})}{V} \quad (51)$$

$$k_{-3} = k_{CH^+\rightarrow TH^+} \quad (52)$$

Acknowledgment. Hervé Lemarchand and David Bensimon are gratefully acknowledged for fruitful discussions. This work was supported by a special grant from the French Ministry of Research in the frame of the Action Concertée Incitative "Physicochimie de la Matière Complexe 2000".

Supporting Information Available: Supporting information regarding sections 2 and 3, including the complete analysis of experimental data; tuning kinetic and thermodynamic properties of reactions using two-site reactants, including kinetic properties, UV−Vis absorption spectra, and determination of proton dissociation constants (PDF). This material is available free of charge via the Internet at http://pubs.acs.org.

References and Notes

(1) Nicolis, G.; Prigogine, I. *Self-Organization in Nonequilibrium Systems*; Wiley: New York, 1977.

(2) Eigen, M.; Schuster, P. *The Hypercycle, A Principle of Natural Self-Organization*; Springer−Verlag: Berlin, Heidelberg, New York, 1979.

(3) Goldbeter, A. *Biochemical Oscillations and Cellular Rhythms*; Cambridge University Press: Cambridge, U.K., 1996.

(4) Jencks, W. P. *Catalysis in Chemistry and Enzymology*; Dover Publications: New York, 1987.

(5) Bachmann, P. A.; Walde, P.; Luisi, P. L.; Lang, J. *J. Am. Chem. Soc.* **1990**, *112*, 8200−8201. Bachmann, P. A.; Walde, P.; Luisi, P. L.; Lang, J. *J. Am. Chem. Soc.* **1991**, *113*, 8204−8209. Bachmann, P. A.; Luisi, P. L.; Lang, J. *Nature* **1992**, *357*, 57−59. Walde, P.; Wick, R.; Fresta, M.; Mangone, A.; Luisi, P. L. *J. Am. Chem. Soc.* **1994**, *116*, 11649−11654.

(6) Buhse, T.; Nagarajan, R.; Lavabre, D.; Micheau, J.-C. *J. Phys. Chem. A* **1997**, *101*, 3910−3917. Buhse, T.; Pimienta, V.; Lavabre, D.; Micheau, J.-C. *J. Phys. Chem. A* **1997**, *101*, 5215−5217. Buhse, T.; Lavabre, D.; Nagarajan, R.; Micheau, J.-C. *J. Phys. Chem. A* **1998**, *102*, 10552−10559. Roque, C.; Pimienta, V.; Lavabre, D.; Micheau, J. C. *Langmuir* **2000**, *16*, 6492−6496. Roque, C.; Pimienta, V.; Lavabre, D.; Micheau, J. C. *J. Phys. Chem. A* **2001**, *105*, 5877−5880.

(7) von Kiedrowski, G. *Angew. Chem., Int. Ed. Engl.*, **1986**, *25*, 932−935. Terfort, A.; von Kiedrowski, G. *Angew. Chem., Int. Ed. Engl.* **1992**, *31*, 654−656. Achilles, T.; von Kiedrowski, G. *Angew. Chem., Int. Ed. Engl.* **1993**, *32*, 1198−1201. Sievers, D.; von Kiedrowski, G. *Nature* **1994**, *369*, 221−224. Luther, A.; Brandsch, R.; von Kiedrowski, G. *Nature* **1998**, *396*, 245−248.

(8) Zielinski, W. S.; Orgel, L. E. *Nature* **1987**, *327*, 346−347. Orgel, L. E. *Acc. Chem. Res.* **1995**, *28*, 109−118.

(9) Li, T.; Nicolaou, K. C. *Nature* **1994**, *369*, 218−221.

(10) Martin, B.; Micura, R.; Pitsch, S.; Eschenmoser, A. *Helv. Chim. Acta* **1997**, *80*, 1901−1951.

(11) Lee, D. H.; Granja, J. R.; Martinez, J. A.; Severin, K.; Ghadiri, M. R. *Nature* **1996**, *382*, 525−528. Lee, D. H.; Severin, K.; Yokobayashi, Y.; Ghadiri, M. R. *Nature* **1997**, *390*, 591−594.

(12) Yao, S.; Ghosh, I.; Zutshi, R.; Chmielewski, J. *Angew. Chem., Int. Ed.* **1998**, *37*, 478−481.

(13) Tjivikua, T.; Ballester, P.; Rebek, J. *J. Am. Chem. Soc.* **1990**, *112*, 1249−1250. Hong, J.-I.; Feng, Q.; Rotello, V.; Rebek, J. *Science* **1992**, *255*, 848−850. Pieters, R. J.; Huc, I.; Rebek, J. *Angew. Chem., Int. Ed. Engl.* **1994**, *33*, 1579−1581.

(14) Reinhoudt, D. N.; Rudkevich, D. M.; de Jong, F. *J. Am. Chem. Soc.* **1996**, *118*, 6880−6889.

(15) Wang, B.; Sutherland, I. O. *Chem. Commun.* **1997**, *16*, 1493−1496.

(16) Soai, K.; Shibata, T.; Morioka, H.; Choji, K. *Nature* **1995**, *378*, 767−768.

(17) Blackmond, D. G.; McMillan, C. R.; Ramdeehul, S.; Schorm, A.; Brown, J. M. *J. Am. Chem. Soc.* **2001**, *123*, 10103−10104.

(18) For an example relying of a photometric origin, see: Borderie, B.; Lavabre, D.; Levy, G.; Micheau, J.-C.; Laplante, J.-P. *J. Am. Chem. Soc.* **1990**, *112*, 4105−4109.

(19) Rebek, J., Jr. *Acc. Chem. Res.* **1984**, *17*, 258−264.

(20) Seeman, J. I. *Chem. Rev.* **1983**, *83*, 83−133.

(21) Leffler, J. E.; Grunwald, E. *Rates and Equilibria of Organic Reactions as Treated by Statistical, Thermodynamic, and Extrathermodynamic Methods*; Dover: New York, 1989.

(22) Jullien, L.; Lemarchand, H. *J. Chem. Educ.* **2001**, *78*, 803−810.

(23) Lemarchand, H.; Guyot, F.; Jousset, L.; Jullien, L. *Thermodynamique de la Chimie*; Hermann: Paris, 1999.

(24) For an illustration of a complex behavior relying on a small range of rate constants, see, for instance: Jullien, L.; Lemarchand, A. *J. Phys. Chem. B* **2001**, *105*, 4415−4423.

(25) Eliel, E. L.; Wilen, S. H.; Mander, L. N. *Stereochemistry of Organic Compounds*; Wiley: New York, Chicester, Brisbane, Toronto, Singapore, **1994**.

(26) Campbell, N.; Henderson, A. W.; Taylor, D. *J. Chem. Soc.* **1953**, 1281−1285.

(27) For other chemical systems involving control by light and pH that could have been considered for experimental illustration, see, for instance: Amellot, M.; Boens, N.; Andriessen, R.; Van der Bergh, V.; De Schryver, F. C. *J. Phys. Chem.* **1991**, *95*, 2041−2047. Pina, F.; Melo, M. J.; Maestri, M.; Ballardini, R.; Balzani, V. *J. Am. Chem. Soc.* **1997**, *119*, 5556−5561.

(28) Shinkai, S.; Shigematsu, K.; Sato, M.; Manabe, O. *J. Chem. Soc., Perkin Trans.* **1982**, 2741−2747.

(29) Eigen, M.; Kruse, W.; Maass, G.; de Mayer, L. *Prog. React. Kinet.* **1964**, *2*, 287−318.

(30) Kresge, A. J. *Acc. Chem. Res.* **1975**, *8*, 354−360.

(31) Bernasconi, C. F. *Acc. Chem. Res.* **1987**, *20*, 301−308.

(32) Eigen, M. *Angew. Chem.* **1963**, *75*, 489−508.

(33) Hill, T. L. *Free Energy Transduction in Biology: The Steady-State Kinetic and Thermodynamic Formalism*; Academic Press: New York, 1977.

(34) Hopfield, J. J. *Proc. Natl. Acad. Sci. U.S.A.* **1974**, *71*, 4135−4139.

(35) Ninio, J. *Biochimie* **1975**, *57*, 587−595.

(36) Yan, J.; Magnasco, M. O.; Marko, J. F. *Nature* **1999**, *401*, 932.

(37) Yan, J.; Magnasco, M. O.; Marko, J. F. *Phys. Rev. E* **2001**, *63*, 031909.

(38) Jullien, L.; Cottet, H.; Hamelin, B.; Jardy, A. *J. Phys. Chem. B* **1999**, *103*, 10866−10875.

(39) Berninger, J.; Krauss, R.; Weinig, H.-G.; Koert, U.; Ziemer, B.; Harms, K. *Eur. J. Org. Chem.* **1999**, 875−884. Krauss, R.; Weinig, H.-G.; Seydack, M.; Bendig, J.; Koert, U. *Angew. Chem., Int. Ed.* **2000**, *39*, 1835−1837. Weinig, H.-G.; Krauss, R.; Seydack, M.; Bendig, J.; Koert, U. *Chem. Eur. J.* **2001**, *7*, 2075−2088. Koert, U.; Krauss, R.; Weinig, H.-G.; Heumann, C.; Ziemer, B.; Mügge, C.; Seydack, M.; Bendig, J. *Eur. J. Org. Chem.* **2001**, 575−586.

(40) Wheeler, O. H.; Gonzalez, D. *Tetrahedron* **1964**, *20*, 189−193.

(41) Frugoni, C. *Gazz. Chim. Ital.* **1957**, *87*, 403−407.

(42) Wang, P. F.; Jullien, L.; Valeur, B.; Filhol, J.-S.; Canceill, J.; Lehn, J.-M. *New J. Chem.* **1996**, *20*, 895−907.